Cavity-free quantum optomechanical cooling by atom-modulated radiation

Hoi-Kwan Lau,* Alexander Eisfeld, and Jan-Michael Rost
Max Planck Institute for the Physics of Complex Systems, Nöthnitzer Straße 38, 01187 Dresden, Germany

(Received 1 August 2018; published 15 October 2018)

We theoretically study the radiation-induced interaction between the mechanical motion of an oscillating mirror and a remotely trapped atomic cloud. When illuminated by continuous-wave radiation, the mirror motion will induce red and blue sideband radiation, which respectively increases and reduces motional excitation. We find that, by suitably driving Λ-level atoms, the mirror correlation with a specific radiation sideband could be converted from the outgoing to the incoming radiation. Thereby, we can manipulate heating and cooling effects. Particularly, we develop an optomechanical cooling strategy that can mutually cancel the heating effect of the outgoing and incoming radiation, rendering the motional ground state attainable by net cooling. Our proposal complements other efforts in quantum cooling of macroscopic objects since it requires neither a cavity nor perfect alignment.

DOI: 10.1103/PhysRevA.98.043827

I. INTRODUCTION

Technological innovation is strongly driven by increasing the precision of mechanical devices while at the same time reducing their size. Fundamentally, the ultimate limit to control mechanical motion is imposed by quantum fluctuation. Reducing motion of a macroscopic object to the quantum limit allows us to build devices with unprecedented precision for detecting gravitational waves [1–4], testing fundamental physics [5,6], quantum information processing [7,8], and more [9,10]. In practice, the motional fluctuation of most devices is orders of magnitude higher than the quantum limit, due to the inevitable coupling to the environment that induces thermal noise.

For over a century, great effort has been spent to tackle thermal noise through advancing cooling techniques [11]. A relatively recent and promising approach is optomechanical cooling, which dissipates motional excitation by converting it to electromagnetic radiation [12–14]. Efficient optomechanical cooling usually requires the mechanical oscillator to be placed in an optical cavity, in order to increase the photon-phonon interaction time. Reduction of motional excitation by orders of magnitude has been demonstrated recently [15,16], and a final excitation at the single phonon level has been achieved [17,18].

Nevertheless, the technical challenges to combine both a high-quality mechanical oscillator and a high-quality radiation cavity compromise the applicability of cavity optomechanical cooling. Given a poor or no cavity at all, one needs to enhance the cooling efficiency by additional mechanisms. Thanks to the versatile techniques developed in atomic control via electromagnetic radiation, coupling a mechanical oscillator to trapped atoms emerges as a promising option. Early proposals suggest a standing wave configuration such that the light beams incoming to and reflected from a mirror are aligned to form an optical lattice atomic trap [19–23]. An effective coupling between the mirror motion and the atomic motional or internal state can be established through photon exchange to remove motional excitation sympathetically by laser cooling of atoms. Recently, some of us have proposed mirror-atom coupling where the incoming and reflected radiation is misaligned and distinct in frequency [24]. By incorporating electromagnetic induced transparency (EIT), the atoms modulate the sideband radiation that is induced by the mirror motion. This effect can be used to amplify or damp the classical oscillation of the mirror.

In this paper, we extend the idea from Ref. [24] to implement optomechanical cooling in the quantum regime. We consider a setup with an oscillating mirror illuminated by two laser beams. The mechanical motion will generate red and blue sidebands in the reflected radiation. Note that each sideband acts differently on motional excitation: the blue sideband is created by beam splitting that cools the mirror, and the red sideband is excited by two-mode squeezing that increases motional excitation.

Remote from the mirror, we consider a cloud of Λ-level atoms which is trapped at the intersection of an incoming and an outgoing laser beam. By driving the atoms appropriately, we find that the mirror correlation with a specific sideband can be converted from the outgoing to the incoming radiation. This allows us to develop two cooling strategies: converting the blue sideband to enhance the cooling effect, or converting the red sideband to suppress the heating effect. We will show that with the latter strategy the mirror can be cooled to the ground motional state.

Our paper is organized as follows. First, the mirror-radiation interaction is discussed in Sec. II followed by an analysis of the dynamics of the trapped atoms in Sec. III. In Sec. IV, we connect the atom and mirror dynamics through a time-local dynamic equation for any system operator. In Sec. V, we discuss two cooling strategies and analyze their

*hklau.physics@gmail.com; current address: Institute for Molecular Engineering, The University of Chicago, 5640 South Ellis Avenue, Chicago, IL 60637, USA.

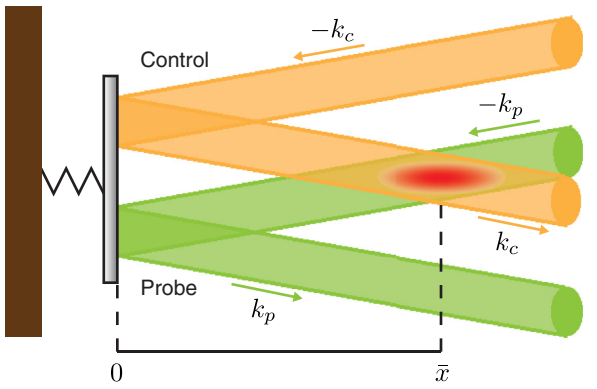

FIG. 1. Configuration of our system. Two radiation beams, Control (upper, orange) and Probe (lower, green), are applied to and reflected from an oscillating mirror. A diluted atomic cloud (red oval) is trapped at the overlap of the outgoing Control and incoming Probe beams.

performance through solving the dynamic equation of motional excitation. In Sec. VI, we briefly discuss the applicability of our scheme to cool realistic oscillators. Conclusions are drawn in Sec. VII.

II. LIGHT-MIRROR INTERACTION

The setup of our system is schematically shown in Fig. 1. An oscillating mirror is illuminated by two beams of continuous-wave (cw) radiation, labeled with Control and Probe, according to the convention of EIT. The Control beam falls directly on the mirror and passes, after reflection from the mirror, through a remotely trapped atomic cloud at distance $\bar{x}$ from the mirror. Conversely, the Probe beam passes through the atomic cloud before hitting the mirror. After reflection it will not be collected but dissipated to the environment. Both the applied Probe ($\beta = p$) and Control ($\beta = c$) beams are described as monochromatic classical light with frequency $\omega_{\beta 0}$ and amplitude $\tilde{\alpha}_\beta$ related to the radiation power via $\mathcal{P}_\beta = |\tilde{\alpha}_\beta|^2 c\hbar\omega_{\beta 0}/(2\pi)$. In the following, these two classical lights will be referred to as Probe and Control drives, respectively.

We consider only the fundamental mode of mirror oscillation. Higher-order modes can be added to the analysis analogously. We model the oscillation with a simple harmonic oscillator of frequency ν and effective mass m. In most systems of interest, the thermal fluctuation of the mirror position is much smaller than the wavelength of the light, so that the incoming and outgoing radiation is dominated by the classical drive. Quantum effects can be incorporated by considering only the leading order of quantum fluctuations.

The Hamiltonian around the mirror surface is given by

$$\begin{aligned} H =& \hbar\nu\hat{b}^\dagger\hat{b} + \sum_{\beta=c,p}\int_{k_{\beta 0}-\kappa}^{k_{\beta 0}+\kappa}\hbar\Delta_\beta(\hat{a}_{k_\beta}^\dagger\hat{a}_{k_\beta} + \hat{a}_{-k_\beta}^\dagger\hat{a}_{-k_\beta})dk_\beta \\ &+ \frac{\hbar}{2}(\mu_p(\hat{a}_p^\dagger - \hat{a}_{-p}^\dagger)(\hat{b}+\hat{b}^\dagger) + \mu_p^*(\hat{b}+\hat{b}^\dagger)(\hat{a}_p - \hat{a}_{-p})) \\ &- \frac{\hbar}{2}(\mu_c(\hat{a}_c^\dagger - \hat{a}_{-c}^\dagger)(\hat{b}+\hat{b}^\dagger) + \mu_c^*(\hat{b}+\hat{b}^\dagger)(\hat{a}_c - \hat{a}_{-c})), \end{aligned} \tag{1}$$

where $k_{p0} \equiv \omega_{p0}/c$ and $k_{c0} \equiv \omega_{c0}/c$. We have assumed that Probe and Control radiation are distinguishable either by sufficiently separated frequencies, or by other degrees of freedom, e.g., polarization. We pick a sufficiently wide frequency domain $2c\kappa$ around each classical drive frequency, i.e., $c\kappa \gg \nu$, so that the collection of radiation modes in each domain can be treated as a continuum; a radiation mode belonging to the continuum around Probe (Control) drive frequency is denoted as a *Probe mode* (*Control mode*). Unless specified, all our integrations over wave vectors will be executed over the respective domain (which has a width of 2κ).

The first term in (1) is the bare Hamiltonian of mirror motion, where $\hat{b}$ is the annihilation operator of the oscillation mode. The second term contains the bare Hamiltonians of the Probe and Control modes. Each of the two modes is characterized by an annihilation operator $\hat{a}_{k_\beta}$, a wave vector k_β, and the detuning from classical drive $\Delta_\beta \equiv c|k_\beta| - \omega_{\beta 0}$. In our setup, the incoming and outgoing modes are almost perpendicular to the mirror surface, but not collinear due to misalignment. The wave vector of each mode is represented by a positive scalar, k_β, and a sign $+$ $(-)$ indicates outgoing (incoming) propagation.

The third and fourth terms in (1) represent the leading-order optomechanical interaction between radiation and mirror motion. This interaction originates from the change of radiation energy density due to mirror motion. Details of the derivation can be found in Appendix A. The interaction strength in each mode is characterized by the factor

$$\mu_\beta \equiv 2\sqrt{\frac{c}{2\pi}}k_{\beta 0}q_0\tilde{\alpha}_\beta, \tag{2}$$

with the quantum fluctuation $q_0 \equiv \sqrt{\hbar/(2m\nu)}$ of the mirror position. For clarity, we denote an annihilation operator with subscript k as a *mode* operator, while that without the subscript k as a *field* operator, which is defined by the transformation

$$\hat{a}_{\pm\beta} \equiv \sqrt{\frac{c}{2\pi}}\int \hat{a}_{\pm k_\beta}dk_\beta. \tag{3}$$

Optomechanical heating and cooling

The optomechanical interaction is usually weak in free-space systems, so the dominant interaction is that on resonance. By using the definition (3), we observe two types of resonant optomechanical interaction in (1). The first type couples the blue sideband modes with the mirror motion in the form of $\hat{a}_k^\dagger\hat{b} + \text{H.c.}$, where the blue sideband wave vector can be $k = \pm(k_{p0} + \nu/c)$ or $\pm(k_{c0} + \nu/c)$. This type of interaction is known as beam splitting (BS), which converts excitation from one mode to another. If the input blue sideband mode is in the vacuum, motional excitation will be converted to photons. The mirror is cooled if the blue sideband mode is not backcoupled.

The second type couples the red sideband mode with the mirror motion in the form of $\hat{a}_k\hat{b} + \text{H.c.}$, where the red sideband wave vector is $k = \pm(k_{p0} - \nu/c)$ or $\pm(k_{c0} - \nu/c)$. This type of interaction is known as two-mode squeezing (TMS) [25]. If the input radiation is in the vacuum, TMS will

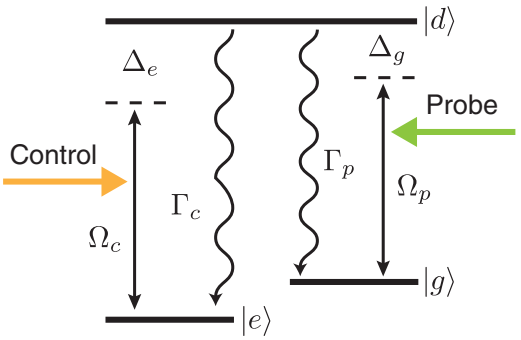

FIG. 2. Level diagram of a Λ-level atom.

create both motional excitation and red sideband photons. The mirror is heated if the red sideband mode is not backcoupled.

To study the dynamics of motional excitation, we apply the input-output formalism [26] to derive the quantum Langevin equation for any mirror operator $\hat{O}_b$,

$$\begin{aligned}\dot{\hat{O}}_b &= \mathcal{L}_b(\hat{O}_b)\\ &\equiv i\nu[\hat{b}^\dagger\hat{b},\hat{O}_b] + \frac{|\mu_p|^2+|\mu_c|^2}{2}\mathcal{D}[\hat{b}+\hat{b}^\dagger](\hat{O}_b)\\ &\quad - i\mu_p\hat{a}_{-p}^{(1)\dagger}[\hat{b}+\hat{b}^\dagger,\hat{O}_b] - i\mu_p^*[\hat{b}+\hat{b}^\dagger,\hat{O}_b]\hat{a}_{-p}^{(1)}\\ &\quad + i\mu_c\hat{a}_{-c}^{\mathrm{in}\dagger}[\hat{b}+\hat{b}^\dagger,\hat{O}_b] + i\mu_c^*[\hat{b}+\hat{b}^\dagger,\hat{O}_b]\hat{a}_{-c}^{\mathrm{in}}, \quad (4)\end{aligned}$$

where $\hat{O}_b$ can be any polynomial of $\hat{b}$ and $\hat{b}^\dagger$; $\hat{a}_{-p}^{(1)\dagger}$ and $\hat{a}_{-c}^{\mathrm{in}\dagger}$ are the input operators of Probe and Control fields, respectively [26]. The dissipator superoperator is defined as $\mathcal{D}[\hat{d}](\hat{O}) \equiv \hat{d}^\dagger\hat{O}\hat{d} - \frac{1}{2}\hat{d}^\dagger\hat{d}\hat{O} - \frac{1}{2}\hat{O}\hat{d}^\dagger\hat{d}$. The incoming Control field is assumed to be vacuum, while the incoming Probe field contains correlation with the trapped atoms.

III. LIGHT-ATOM INTERACTION

We consider a cloud of atoms trapped remotely from the mirror. For each atom, we utilize only two metastable states, $|g\rangle$ and $|e\rangle$, and one quickly-decaying state $|d\rangle$. The atomic states are arranged in a Λ configuration, as shown in Fig. 2. The $|g\rangle \leftrightarrow |d\rangle$ and $|e\rangle \leftrightarrow |d\rangle$ transitions are driven by the incoming Probe and outgoing Control drives, respectively. The total Hamiltonian of the atomic cloud and the radiation is

$$H_{\mathrm{total}} = H_{\mathrm{rad}} + \sum_{i=1}^{N}\left(H_a^{(i)} + H_b^{(i)} + H_I^{(i)} + H_{Ib}^{(i)}\right). \quad (5)$$

$H_{\mathrm{rad}} = \int \hbar\Delta_p\hat{a}_{-k_p}^\dagger\hat{a}_{-k_p}dk_p + \int \hbar\Delta_c\hat{a}_{k_c}^\dagger\hat{a}_{k_c}dk_c$ is the bare Hamiltonian of the incoming Probe and outgoing Control modes. N is the total number of atoms. $H_a^{(i)}$ is the Hamiltonian for the ith atom,

$$\begin{aligned}H_a^{(i)} &= -\hbar\Delta_g\sigma_{gg}^{(i)} - \hbar\Delta_e\sigma_{ee}^{(i)} + i\hbar\frac{\Omega_p^{(i)*}}{2}\sigma_{gd}^{(i)} - i\hbar\frac{\Omega_p^{(i)}}{2}\sigma_{dg}^{(i)}\\ &\quad + i\hbar\frac{\Omega_c^{(i)*}}{2}\sigma_{ed}^{(i)} - i\hbar\frac{\Omega_c^{(i)}}{2}\sigma_{de}^{(i)}, \quad (6)\end{aligned}$$

where Δ_g (Δ_e) is the detuning of the $|g\rangle \leftrightarrow |d\rangle$ ($|e\rangle \leftrightarrow |d\rangle$) transition from the Probe (Control) drive frequencies. The Rabi frequency $\Omega_\beta^{(i)}$ is the same in magnitude $\Omega_\beta = \sqrt{2c\gamma_\beta/\pi}\tilde{\alpha}_\beta$ for all atoms i, but differs in phase $\phi_{\beta i} \equiv s_\beta k_{\beta 0}x_i$, where $s_p = -1$ and $s_c = 1$, which depends on the atomic position x_i, i.e., $\Omega_\beta^{(i)} = e^{i\phi_{\beta i}}\Omega_\beta$. The atomic coherence operator is $\sigma_{ll'}^{(i)} \equiv |l^{(i)}\rangle\langle l'^{(i)}|$, where $|l^{(i)}\rangle$ is the $|l\rangle$ state of the ith atom. $H_I^{(i)}$ is the interaction between the atom and Probe and Control modes,

$$\begin{aligned}H_I^{(i)} &= i\hbar\sqrt{\frac{c\gamma_p}{2\pi}}\int e^{ik_px_i}\hat{a}_{-k_p}^\dagger\sigma_{gd}^{(i)} - e^{-ik_px_i}\sigma_{dg}^{(i)}\hat{a}_{-k_p}dk_p\\ &\quad + i\hbar\sqrt{\frac{c\gamma_c}{2\pi}}\int e^{-ik_cx_i}\hat{a}_{k_c}^\dagger\sigma_{ed}^{(i)} - e^{ik_cx_i}\sigma_{de}^{(i)}\hat{a}_{k_c}dk_c,\end{aligned}$$

where γ_p and γ_c are the decay rates to the Probe and Control modes, respectively. $H_b^{(i)}$ is the bare Hamiltonian of the bath modes; $H_{Ib}^{(i)}$ is the atom-bath interaction that induces atomic decay. Here, we have assumed that the atomic cloud is dilute and each atom is coupled to an independent bath.

After integrating the Heisenberg equation for the field operators and applying standard approximations [26], we arrive at the Langevin equation for any atomic operator $\sigma^{(i)}$,

$$\begin{aligned}\dot{\sigma}^{(i)} &= \mathcal{L}_a^{(i)}(\sigma^{(i)})\\ &\equiv \frac{i}{\hbar}\left[H_a^{(i)},\sigma^{(i)}\right]\\ &\quad + (\gamma_p+\Gamma_p)\mathcal{D}\left[\sigma_{gd}^{(i)}\right](\sigma^{(i)}) + (\gamma_c+\Gamma_c)\mathcal{D}\left[\sigma_{ed}^{(i)}\right](\sigma^{(i)})\\ &\quad - \sqrt{\gamma_p}e^{i\phi_{pi}}\hat{a}_{-p}^{(i+1)\dagger}\left(t+\frac{x_i}{c}\right)\left[\sigma_{gd}^{(i)},\sigma^{(i)}\right]\\ &\quad + \sqrt{\gamma_p}e^{-i\phi_{pi}}\left[\sigma_{dg}^{(i)},\sigma^{(i)}\right]\hat{a}_{-p}^{(i+1)}\left(t+\frac{x_i}{c}\right)\\ &\quad - \sqrt{\gamma_c}e^{-i\phi_{ci}}\hat{a}_c^{(i)\dagger}\left(t-\frac{x_i}{c}\right)\left[\sigma_{ed}^{(i)},\sigma^{(i)}\right]\\ &\quad + \sqrt{\gamma_c}e^{i\phi_{ci}}\left[\sigma_{de}^{(i)},\sigma^{(i)}\right]\hat{a}_c^{(i)}\left(t-\frac{x_i}{c}\right)\\ &\quad - \sqrt{\Gamma_p}\left(\hat{r}_p^{\mathrm{in}(i)\dagger}\left[\sigma_{gd}^{(i)},\sigma^{(i)}\right] - \left[\sigma_{dg}^{(i)},\sigma^{(i)}\right]\hat{r}_p^{\mathrm{in}(i)}\right)\\ &\quad - \sqrt{\Gamma_c}\left(\hat{r}_c^{\mathrm{in}(i)\dagger}\left[\sigma_{ed}^{(i)},\sigma^{(i)}\right] - \left[\sigma_{de}^{(i)},\sigma^{(i)}\right]\hat{r}_c^{\mathrm{in}(i)}\right), \quad (7)\end{aligned}$$

where the index of an atom, i, is arranged according to its distance from the mirror. If not explicitly indicated, the operators are evaluated at time t. Γ_p and Γ_c are the spontaneous decay rates from $|d\rangle$ to $|g\rangle$ and $|e\rangle$, respectively, and $\hat{r}_p^{\mathrm{in}(i)}$ and $\hat{r}_c^{\mathrm{in}(i)}$ are the input field operators of the bath that is responsible for the respective decay. $\hat{a}_{-p}^{(i)}$ and $\hat{a}_c^{(i)}$ are the Probe and Control input field operators between the ith and $(i-1)$th atom,

$$\hat{a}_{-p}^{(i)} \equiv \hat{a}_{-p}^{\mathrm{in}} + \mathcal{A}_p^{(i)}, \quad \hat{a}_c^{(i)} \equiv \hat{a}_c^{(1)} + \mathcal{A}_c^{(i)}, \quad (8a)$$

with the collective atomic operators

$$\mathcal{A}_p^{(i)}(t) \equiv \sqrt{\gamma_p}\sum_{j=i}^{N} e^{i\phi_{pi}}\sigma_{gd}^{(j)}\left(t-\frac{x_j}{c}\right), \quad (8b)$$

$$\mathcal{A}_c^{(i)}(t) \equiv \sqrt{\gamma_c}\sum_{j=1}^{i-1} e^{-i\phi_{ci}}\sigma_{ed}^{(j)}\left(t+\frac{x_j}{c}\right). \quad (8c)$$

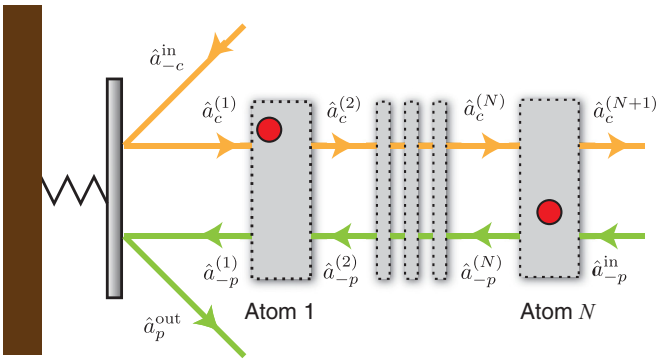

FIG. 3. Atomic cloud is modeled as an array of atom that the radiation passes through each in sequence. For a general atomic cloud, we can divide the cloud into parallel slices (gray rectangles), and each slice consists of a negligible number of atoms. For simplicity, in this work we consider each slice contains exactly one atom and the slices are indexed according to the distance from the mirror. Our model remains valid if the atoms in each slice are weakly interacting, which is a usual assumption for diluted cloud.

The arrangement of the atoms and field operators is shown in Fig. 3.

For each atom, the influence from the classical drive is much stronger than that from the sidebands and other atoms. Therefore, the equilibrium state of each atom is well approximated by its bare steady state. When $\Delta_g = \Delta_e \equiv \Delta$, the bare steady state of a Λ-level atom,

$$|\text{DS}^{(i)}\rangle = \frac{\Omega_c^{(i)}}{\sqrt{|\Omega_p|^2+|\Omega_c|^2}}|g^{(i)}\rangle - \frac{\Omega_p^{(i)}}{\sqrt{|\Omega_p|^2+|\Omega_c|^2}}|e^{(i)}\rangle, \tag{9}$$

is a dark state, because the radiation transition component vanishes, i.e., $\langle \text{DS}^{(i)}|\sigma_{gd}^{(i)}|\text{DS}^{(i)}\rangle = \langle \text{DS}^{(i)}|\sigma_{ed}^{(i)}|\text{DS}^{(i)}\rangle = 0$.

As we will discuss, our cooling scheme requires the manipulation of mirror motion correlation with the radiation sidebands. If the atomic bare steady state is not dark, a significant fraction of Probe and Control radiation will be scattered to the bath and lost. Such loss will reduce the cooling efficiency. Therefore, our studies focus on the choice of atomic parameters that render the bare steady state dark. When the sideband and other atoms are considered, their influence on the atom can be treated as a perturbation on the bare steady state.

IV. RADIATION-MEDIATED ATOM-MIRROR INTERACTION

In our setup, the reflected Control field will contain correlation with the mirror motion. Subsequently, it interacts with the atomic cloud, which in-turn modulates the Probe field. Finally, the Probe field carries the correlation contained in the atoms when falling on the mirror. Overall, the mirror and the atomic cloud form a cascaded quantum system that is connected by radiation.

The dynamics of such cascaded quantum system can be studied by imposing the following input-output relations as the boundary conditions of Eqs. (4) and (7):

$$\hat{a}_c^{(1)}(t) = -\hat{a}_{-c}^{\text{in}}(t) + \frac{i\mu_c}{2}(\hat{b}(t)+\hat{b}^\dagger(t)), \tag{10a}$$

$$\hat{a}_{-p}^{(1)}(t) = \hat{a}_{-p}^{\text{in}}(t) + \mathcal{A}_p^{(1)}(t). \tag{10b}$$

Then any operator composition of mirror and atomic operators, e.g., $\hat{O} \equiv \hat{O}_b \otimes \sigma^{(i)}$, follows the combined master equation $\dot{\hat{O}} = \mathcal{L}_b(\hat{O}) + \mathcal{L}_a^{(i)}(\hat{O})$ [26].

Due to the dependence of the Heisenberg operators on different instances of time, e.g., the field operator in the fourth line of (7), the combined master equation is technically difficult to solve. These time shifts appear because it take the light a finite time to travel between the atoms and mirror. Nevertheless, in our regime of interest the time dependence can be approximated to be uniform as we will see now.

First, the Probe field that carries information of atom i from time $t - x_i/c$ interacts with the mirror at time t. Uniform dependence on t can be achieved by simply rewriting (7) in terms of the advanced atomic operator $\tilde{\sigma}^{(i)}(t) \equiv \sigma^{(i)}(t - x_i/c)$ [26].

Second, the Control field which interacts with atom i at time $t - x_i/c$ carries mirror information from time $t - 2x_i/c$. In combination with the effect of the Probe field, this interaction effectively correlates the mirror properties at time $t - 2x_i/c$ with that at time t. Since the mirror motion is dominated by its bare Hamiltonian, we may approximate the mirror operator as $\hat{b}(t - 2x_i/c) \approx e^{i\nu 2x_i/c}\hat{b}(t)$.

Third, we consider a small atomic cloud implying that the light traveling time within the cloud is much shorter than the atomic and mirror time scale, i.e., $\frac{|x_N - x_1|}{c} \ll \min\{1/\nu, 1/\Gamma, 1/\Omega\}$. This allows all atoms to approximately share the same time dependence, i.e., $\sigma(t - \frac{x_i - x_j}{c}) \approx \sigma(t)$. We leave the explicit form of the resulting time-local combined master equation to Appendix C.

V. COOLING STRATEGY

Using the time-local combined master equation for $\hat{O} = \hat{b}^\dagger\hat{b}$, we obtain the dynamic equation for the mean motional excitation,

$$\frac{d}{dt}\langle\hat{b}^\dagger\hat{b}\rangle = \Lambda_{\text{rad}} - i\mu_p\langle\mathcal{A}_p^{(1)\dagger}(\hat{b}-\hat{b}^\dagger)\rangle - i\mu_p^*\langle(\hat{b}-\hat{b}^\dagger)\mathcal{A}_p^{(1)}\rangle. \tag{11a}$$

The first rate, which is given by

$$\Lambda_{\text{rad}} = \frac{|\mu_p|^2+|\mu_c|^2}{2}, \tag{11b}$$

is induced only by classical drives but not the atoms. This rate is always positive and therefore contributes to heating due to the fact that TMS heating is stronger than BS cooling in optomechanical interactions. The terms proportional to $\langle\hat{b}\mathcal{A}_p^{(1)}\rangle$ and $\langle\hat{b}^\dagger\mathcal{A}_p^{(1)}\rangle$ represent different types of atom-induced optomechanical interaction; see (8b). Because $\hat{b}$ roughly oscillates at $e^{-i\nu t}$, the zero-frequency component of $\langle\hat{b}\mathcal{A}_p^{(1)}\rangle$ is dominated by the $e^{i\nu t}$ component of $\mathcal{A}_p^{(1)}$. According to (10b), this frequency component contributes to the red sideband Probe mode. Since the red sideband interacts with mirror

through TMS, the zero-frequency component of $\langle \hat{b}\mathcal{A}_p^{(1)}\rangle$ can be viewed as an atom-induced TMS interaction. Similarly, the zero-frequency component of $\langle \hat{b}^\dagger\mathcal{A}_p^{(1)}\rangle$ corresponds to the atom-induced BS interaction.

To quantify the atomic contributions, we construct the master equation for $\hat{O} = \hat{b}\otimes\sigma^{(i)}$ and $\hat{b}^\dagger\otimes\sigma^{(i)}$. In our regime of weak optomechanical interaction, the expectation value of these operators can be approximated by a Floquet series expansion in motional frequency, i.e., $\langle\hat{O}(t)\rangle \approx \sum_n \langle\hat{O}\rangle_n(t)e^{in\nu t}$, where $\langle\hat{O}\rangle_n(t)$ varies on a time scale much slower than $1/\nu$. Since the bare dynamics of motional excitation is much slower than the oscillation frequency, we consider the dominant atomic effect on motional excitation is given by the zero-frequency components, i.e., $\langle\hat{O}\rangle_0$. After summing the contributions of each atom, we obtain the recurrence relation

$$\langle \hat{b}\mathcal{A}_p^{(i)}\rangle_0 = (1+|\tilde{\alpha}_c|^2J(-\nu))\langle \hat{b}\mathcal{A}_p^{(i+1)}\rangle_0 - \tilde{\alpha}_p\tilde{\alpha}_c^* J(-\nu)\langle \hat{b}\mathcal{A}_c^{(i)}\rangle_0 - i\,e^{-i\nu\tau}\frac{\mu_c}{2}\tilde{\alpha}_p\tilde{\alpha}_c^* J(-\nu)\langle\hat{b}\hat{b}^\dagger\rangle, \tag{12a}$$

$$\langle \hat{b}\mathcal{A}_c^{(i+1)}\rangle_0 = -\tilde{\alpha}_p^*\tilde{\alpha}_c J(-\nu)\langle \hat{b}\mathcal{A}_p^{(i+1)}\rangle_0 + (1+|\tilde{\alpha}_p|^2J(-\nu))\langle \hat{b}\mathcal{A}_c^{(i)}\rangle_0 + i\,e^{-i\nu\tau}\frac{\mu_c}{2}|\tilde{\alpha}_p|^2 J(-\nu)\langle\hat{b}\hat{b}^\dagger\rangle, \tag{12b}$$

$$\langle \hat{b}^\dagger\mathcal{A}_p^{(i)}\rangle_0 = (1+|\tilde{\alpha}_c|^2J(\nu))\langle \hat{b}^\dagger\mathcal{A}_p^{(i+1)}\rangle_0 - \tilde{\alpha}_p\tilde{\alpha}_c^* J(\nu)\langle \hat{b}^\dagger\mathcal{A}_c^{(i)}\rangle_0 - i\,e^{i\nu\tau}\frac{\mu_c}{2}\tilde{\alpha}_p\tilde{\alpha}_c^* J(\nu)\langle\hat{b}^\dagger\hat{b}\rangle, \tag{12c}$$

$$\langle \hat{b}^\dagger\mathcal{A}_c^{(i+1)}\rangle_0 = -\tilde{\alpha}_p^*\tilde{\alpha}_c J(\nu)\langle \hat{b}^\dagger\mathcal{A}_p^{(i+1)}\rangle_0 + (1+|\tilde{\alpha}_p|^2J(\nu))\langle \hat{b}^\dagger\mathcal{A}_c^{(i)}\rangle_0 + i\,e^{i\nu\tau}\frac{\mu_c}{2}|\tilde{\alpha}_p|^2 J(\nu)\langle\hat{b}^\dagger\hat{b}\rangle, \tag{12d}$$

with the round-trip traveling time $\tau \equiv 2\bar{x}/c$ of light between the mirror and the atomic cloud, where $\bar{x} = \sum_i x_i/N$ is the mean distance of the atoms from the mirror. The spectral factor reads

$$J(\omega) = \frac{\gamma_p\gamma_c}{2\pi}\frac{i16\omega c}{(|\Omega_p|^2+|\Omega_c|^2)[-2i\omega(\gamma_p+\Gamma_p+\gamma_c+\Gamma_c)+4\Delta\omega-4\omega^2+|\Omega_p|^2+|\Omega_c|^2]}. \tag{13}$$

The derivation of this recurrence relation is given in Appendix D.

Equations (12a),(12b) and Eqs. (12c),(12d) form two systems of equation that can be solved separately. For simplicity, we consider the same amplitudes for both Probe and Control drives, i.e., $\tilde{\alpha}_p = \tilde{\alpha}_c \equiv \tilde{\alpha}$. As discussed in Appendix F, it is in fact the optimal choice of driving amplitudes that produces the minimum steady-state motional excitation. Before presenting the solution, we discuss the physics underneath. By adding (12a) to (12b), and (12c) to (12d), we get the relations

$$\langle \hat{b}\mathcal{A}_p^{(i)}\rangle_0 - \langle \hat{b}\mathcal{A}_p^{(i+1)}\rangle_0 = -\langle \hat{b}\mathcal{A}_c^{(i+1)}\rangle_0 + \langle \hat{b}\mathcal{A}_c^{(i)}\rangle_0, \tag{14}$$

$$\langle \hat{b}^\dagger\mathcal{A}_p^{(i)}\rangle_0 - \langle \hat{b}^\dagger\mathcal{A}_p^{(i+1)}\rangle_0 = -\langle \hat{b}^\dagger\mathcal{A}_c^{(i+1)}\rangle_0 + \langle \hat{b}^\dagger\mathcal{A}_c^{(i)}\rangle_0. \tag{15}$$

According to Eqs. (8a) and (8b), and the fact that $\hat{b}$ varies roughly as $e^{i\nu t}$, Eq. (14) describes the changes of the red sideband modes of Probe and Control after interacting with the ith atom. More explicitly, a reduction of correlations between outgoing Control mode and the mirror will be the same as an increase of correlations between incoming Probe mode and the mirror. This can be interpreted as a conversion of the correlation with the mirror from the outgoing Control mode to the incoming Probe mode. Subsequently, the Probe red sideband will bring the correlation back to the mirror and affect the TMS interaction. The analogous phenomenon is described by (15), where the mirror correlation with the blue sideband mode is converted from outgoing Control to incoming Probe. This correlation will then affect the BS interaction.

Following the procedure in Appendix E, we obtain the solution for Eqs. (12a)–(12d) as

$$\langle \hat{b}\mathcal{A}_p^{(1)}\rangle_0 = -e^{-i\nu\tau}\frac{i\mu_c}{2}\mathcal{S}(-\nu)\langle\hat{b}\hat{b}^\dagger\rangle, \tag{16a}$$

$$\langle \hat{b}^\dagger\mathcal{A}_p^{(1)}\rangle_0 = -e^{i\nu\tau}\frac{i\mu_c}{2}\mathcal{S}(\nu)\langle\hat{b}^\dagger\hat{b}\rangle, \tag{16b}$$

with

$$\mathcal{S}(\omega) = \frac{N|\tilde{\alpha}|^2J(\omega)}{1-N|\tilde{\alpha}|^2J(\omega)}. \tag{16c}$$

When substituting (16) into (11a), we obtain the main result of our work: a dynamic equation for the mean motional excitation,

$$\frac{d}{dt}\langle\hat{n}\rangle = \Lambda_{\rm rad} + \Lambda_+\langle\hat{n}\rangle + \Lambda_-(\langle\hat{n}\rangle+1), \tag{17}$$

with the heating rate $\Lambda_{\rm rad}$ from (11b), the phonon number operator $\hat{n}\equiv\hat{b}^\dagger\hat{b}$, and

$$\Lambda_\pm \equiv \pm{\rm Re}[e^{\pm i\nu\tau}\mu_p^*\mu_c\mathcal{S}(\pm\nu)]. \tag{18}$$

Atom-induced BS contributes Λ_+, and Λ_- comes from atom-induced TMS. The atoms induce a net cooling effect of the mirror if $\Lambda_+ + \Lambda_- < 0$. In this case, the residual motional excitation at the steady state, $d\langle\hat{n}\rangle/dt = 0$, is

$$\langle\hat{n}\rangle_{\rm ss} = -\frac{\Lambda_{\rm rad}+\Lambda_-}{\Lambda_++\Lambda_-}, \tag{19}$$

where the subscript ss denotes the steady state.

The sign of $(\Lambda_+ + \Lambda_-)$ is determined by the phase, $e^{i\nu\tau}$, as well as the relative importance of the atom-induced effects, of which the magnitude is characterized by the spectral factor $J(\omega)$. In practice, the phase can be manipulated by choosing the position of the atomic cloud, and the spectral factor can be engineered by adjusting atomic parameters.

For our purpose of cooling, we explore system parameters that could implement either of the mechanisms: enhancing cooling effect of BS or suppressing heating effect due to TMS. Figure 4 illustrates our cooling strategies. In the following, we

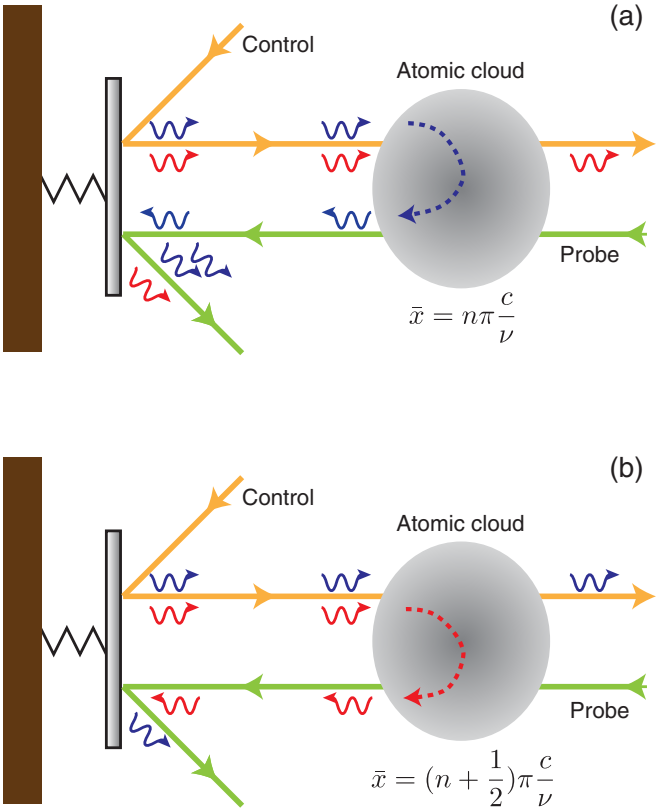

FIG. 4. Illustration of cooling strategies. (a) BS-enhancing strategy: atomic parameters are chosen to convert blue sideband correlation with mirror from outgoing Control to incoming Probe. The correlation contained by the Probe mode will enhance the BS cooling effect. Nevertheless, red sideband of both outgoing Control and outgoing Probe will be dissipated and induce TMS heating. (b) TMS-suppressing strategy: atomic parameters are chosen to convert red sideband correlation with mirror from outgoing Control to incoming Probe. Due to a time delay, the correlation contained by the Probe mode will suppress TMS heating. However, blue sideband of both Control and Probe is unaffected. Its dissipation will induce net cooling on the mirror.

will show that, while both mechanisms can induce cooling, the motional ground state cannot be reached by enhancing BS alone. Ground-state cooling requires optimally chosen system parameters to fully suppress the TMS heating effect.

A. Enhancing beam splitting

First, we study the cooling strategy with an atom-enhanced BS interaction. In this case, the net cooling rate is dominated by a negative Λ_+. From (13), we learn that $J(\omega)$, and hence $\mathcal{S}(\omega)$, always have a negative real part. Therefore, Λ_+ is always negative if $e^{i\nu\tau} = 1$. Such criterion could be satisfied by placing the atomic cloud close to the mirror, i.e., $\bar{x} \approx 0$, or generally for $\bar{x} = n\pi\frac{c}{\nu}$.

On the other hand, at this position the atom-induced TMS always contributes to heating, i.e., $\Lambda_- > 0$. Achieving a net cooling rate thus requires enhancing the BS effect, i.e., $|\Lambda_+| \gg |\Lambda_-|$. This can be achieved by introducing a frequency asymmetry in the spectral factor, i.e., $|J(\nu)| \gg |J(-\nu)|$. As in EIT cooling [27,28], such asymmetry can be

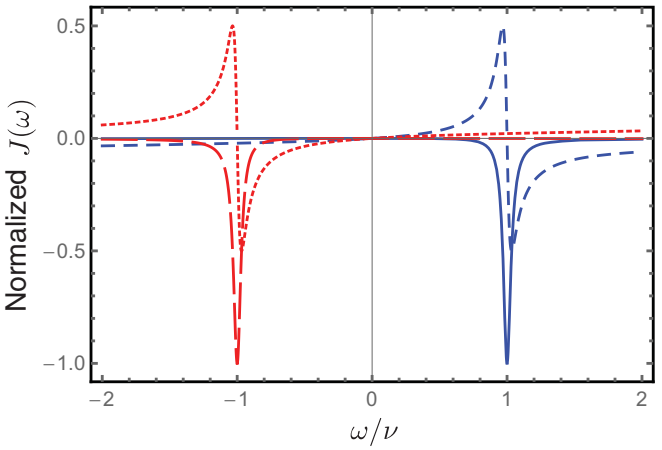

FIG. 5. Typical behavior of spectral function $J(\omega)$. Blue: real (solid) and imaginary (dashed) part of $J(\omega)/|J(\nu)|$. The parameters are $\Omega_p = \Omega_c = 4\nu$ and $\gamma_p + \Gamma_p = \gamma_c + \Gamma_c = 0.3\nu$. The detuning Δ is chosen to satisfy (20), in order to facilitate the atom interaction with blue sideband radiation. The interaction with red sideband is suppressed, as we can see $|J(\nu)| \gg |J(-\nu)|$. Red: real (long-dashed) and imaginary (dotted) part of $J(\omega)/|J(-\nu)|$, of which the atomic parameters are the same as those of the blue lines, except Δ is chosen to satisfy (23).

produced by using sufficiently large Rabi frequencies, i.e., $|\Omega_p|^2 + |\Omega_c|^2 \gg \nu(\gamma_p + \Gamma_p + \gamma_c + \Gamma_c)$, and by choosing a detuning that satisfies

$$4\Delta\nu - 4\nu^2 + |\Omega_p|^2 + |\Omega_c|^2 = 0. \tag{20}$$

The typical behavior of such a $J(\omega)$ is shown with blue lines in Fig. 5.

1. Few atom regime

In the regime of small number of atoms, i.e., $N|\tilde{\alpha}|^2|J(\omega)| \ll 1$ for all ω, the net cooling rate can be approximated as

$$\Lambda_+ + \Lambda_- \approx N|\tilde{\alpha}|^2\mu_p^*\mu_c \mathrm{Re}[J(\nu) - J(-\nu)]. \tag{21}$$

According to (2), $\mu_p^*\mu_c$ is real and positive under our assumption $\tilde{\alpha}_p = \tilde{\alpha}_c$. It is easy to show that $\Lambda_+ + \Lambda_- < 0$, and so the mirror is cooled in this setup.

In fact, the same setup is studied in Ref. [24], where the cooling rate (21) is derived using semiclassical techniques. However, the few-atom assumption implies that the atom-induced cooling is always much weaker than the heating induced by the classical drives, i.e., $\Lambda_{\mathrm{rad}} \gg |\Lambda_+|$. Unnoticed in Ref. [24], the residual motional excitation in this setup is thus enormous, i.e., $\langle\hat{n}\rangle_{\mathrm{ss}} \gg 1$.

2. Many atom regime

In order to improve the cooling rate, we take the number of atoms so large that $N|\tilde{\alpha}|^2|J(\nu)| \gg 1 \gg N|\tilde{\alpha}|^2|J(-\nu)|$ is satisfied. In this regime, the atom-induced BS effect is saturated as $\Lambda_+ \approx -\mu_p^*\mu_c$, while $\Lambda_- \approx -N|\tilde{\alpha}|^2\mu_p^*\mu_c \mathrm{Re}(J(-\nu))$ is small due to an asymmetric spectral function. The

steady-state motional excitation is

$$\langle\hat{n}\rangle_{\rm ss} \approx \frac{\Lambda_{\rm rad}}{\mu_p^*\mu_c} \geqslant 1, \tag{22}$$

where the last relation follows from the Cauchy-Schwarz inequality.

Equation (22) shows that even with the optimal choice of system parameters, enhancing the BS cooling effect can only cool the mirror to a thermal state with unity motional excitation. This can be understood realizing that BS interaction is ineffective to convert motional excitation to the blue sideband, when the mirror is close to motional ground state. On the other hand, TMS induces excitation even if the red sideband mode is in vacuum. As a result, the motional ground state cannot be a steady state unless TMS is suppressed.

B. Suppressing two-mode squeezing

To pursue ground-state cooling, we consider another cooling strategy that aims to suppress the TMS heating effect. In this case, the net cooling rate will be dominated by a negative Λ_-. This is achievable if the atomic cloud is placed at a distance $\bar{x} = (n + \frac{1}{2})\pi\frac{c}{\nu}$ from the mirror, so that $e^{i\nu\tau} = -1$.

At this position, the atom-induced BS reduces the cooling efficiency, i.e., $\Lambda_+ > 0$. A net cooling rate can be attained by engineering an asymmetric spectral factor $|J(-\nu)| \gg |J(\nu)|$, which leads to $|\Lambda_-| \gg |\Lambda_+|$. Similar to the choice of parameters in Sec. V A, such asymmetry can be achieved by using large Rabi frequencies, but choosing a detuning that satisfies

$$-4\Delta\nu - 4\nu^2 + |\Omega_p|^2 + |\Omega_c|^2 = 0 \tag{23}$$

instead of (20). The typical behavior of this $J(\omega)$ is shown with red lines in Fig. 5.

In the many-atom regime $N|\tilde{\alpha}|^2|J(-\nu)| \gg 1 \gg N|\tilde{\alpha}|^2|J(\nu)|$, we have $\Lambda_- \approx -\mu_p^*\mu_c$ and $\Lambda_+ \approx -N|\tilde{\alpha}|^2\mu_p^*\mu_c{\rm Re}(J(\nu))$. The atom-induced TMS interaction is saturated, but $|\Lambda_+|$ is small due to the spectral factor asymmetry. The steady-state motional excitation is given by

$$\langle\hat{n}\rangle_{\rm ss} \approx \frac{\Lambda_{\rm rad}}{\mu_p^*\mu_c} - 1 \geqslant 0. \tag{24}$$

In contrast to the BS-enhancing strategy, the TMS-suppressing strategy can reach the motional ground steady state if $\mu_p = \mu_c$. According to (2), this can be fulfilled by choosing two atomic state transitions with similar energy, so that the classical drive frequency is roughly the same, $\omega_{p0} \approx \omega_{c0}$ [29].

We now explain the principle behind this strategy. At the beginning, the Control red sideband couples to the mirror motion through TMS interaction. If this sideband is lost, motional excitation will increase. Therefore, we choose the system parameters, such that the mirror correlation with the outgoing Control red sideband is completely transferred to the incoming Probe.

The crucial trick of our strategy is that the round-trip traveling time is chosen to satisfy $e^{i\nu\tau} = -1$. When the Probe field reaches the mirror, the mirror motion is π phase behind that at the beginning. This π phase effectively inverts the sign of the TMS Hamiltonian, so the mirror and Probe red sideband undergo an anti-TMS interaction. If the optomechanical interaction strength is the same for Probe and Control field, i.e., $\mu_p = \mu_c$, the anti-TMS can completely "undo" the mirror-Control TMS. Therefore, the TMS heating effect is fully suppressed.

On the other hand, because $|\Lambda_+|$ is kept small, the BS cooling effect of the blue sideband is barely affected by the atoms, so the mirror experiences a net cooling. Without TMS heating, the motional ground state is attainable at the steady state.

We note that the heating effect due to the two-mode-squeezing interaction is an ubiquitous problem in optomechanical cooling, i.e., in both cavity and cavity-free systems. In cavity optomechanics (CO), such process imposes the quantum backaction limit that lower bounds the steady-state phonon occupation [12,13]. Numerous efforts have been proposed and implemented to evade the backaction limit in CO, such as by injecting squeezed light [30,31] or by measurement feedback [32]. Particularly, our method of TMS suppression resembles the CO strategy of quantum noise interference [33]. The principle is that, apart from the optomechanical coupling to the heating red sideband, the mechanical oscillator is coupled by an additional dissipative channel to the same sideband. By tuning the additional coupling, the dissipative channels can be made to destructively interfere; hence the heating effect is suppressed. In CO, the additional channel can be realized by introducing dissipative coupling [33], intracavity atomic ensembles [34,35], doped quantum emitters [36,37], interferometer [16,38], and coupling to additional mechanical oscillators [39]. In our cavity-free system, TMS heating is induced by the dissipation of the reflected probe red sideband through the channel "mirror → outgoing Probe." The inclusion of remotely trapped atoms can be viewed as an introduction of a new channel, i.e., excitation is transferred through "mirror → outgoing Control → atom → incoming Probe → outgoing Probe." By choosing the appropriate atomic parameters and position, the two dissipative channels destructively interfere and suppress the red sideband heating.

VI. PRACTICAL IMPLEMENTATION

Finally, we discuss the practicality of our scheme in cooling the realistic mechanical oscillator. We first include environmental heating to the dynamic equation,

$$\langle\dot{\hat{n}}\rangle = -\left(|\mu|^2 + \frac{\nu}{Q}\right)\langle\hat{n}\rangle + \frac{\nu}{Q}\mathcal{N}_{\rm th}. \tag{25}$$

Q is the quality factor of the oscillator, which is defined as the number of oscillation periods to lose one-half motional excitation if the environment is at zero temperature. $\mathcal{N}_{\rm th} \approx \frac{k_B T}{\hbar\nu}$ is the motional excitation at thermal equilibrium. For simplicity, we have picked the optimal optomechanical strength $\mu_p \approx \mu_c = \mu$, and assumed $\Lambda_+ \to 0$ is suppressed by appropriately chosen system parameters.

As an example, we consider a state-of-the-art mechanical oscillator reported in Ref. [40]. This is a single-crystal diamond cantilever with length 240 μm, width 12 μm, thickness 0.66 μm, oscillation frequency $\nu \approx 2\pi \times 32$ kHz, and quality factor $Q \approx 1.5 \times 10^6$.

The remotely trapped atoms are chosen to be rubidium 85. The atomic transition employed is the D_2 line, i.e., $5^2S_{1/2} \leftrightarrow 5^2P_{3/2}$, which couples to the radiation of wavelength $\approx$780 nm [41]. The Probe and Control fields can be differentiated by different polarization of transitions, or by hyperfine-state energy shift due to external static magnetic field.

In a 10 mK environment, which is achievable by state-of-the-art cryogenic techniques [11], implementing our cooling scheme with a cw laser power of $\mathcal{P} = 10\,\mathrm{mW}$ could reduce the motional excitation from initially $\langle\hat{n}\rangle(t=0) = \mathcal{N}_{\mathrm{th}} \approx 6500$ to a quantum level steady state, $\langle\hat{n}\rangle_{\mathrm{ss}} \approx 2$. At this level of motional excitation, the oscillator can already be used for a variety of applications, such as detecting macroscopic nonclassicality [42] or quantum computation [43].

The steady-state motional excitation can be further reduced by, e.g., enhancing the power of the cw laser, reducing the environmental temperature, or increasing the zero-point position fluctuation by using a lower-frequency oscillator.

VII. CONCLUSION

In this work, we have studied the radiation-induced interaction between remotely trapped atoms and the motion of a mirror. Considering a cavity-free setup with the mirror driven by two continuous-wave beams, Control and Probe, we have identified the resonant optomechanical interaction either as beam splitting with the blue radiation sideband or two-mode squeezing with the red radiation sideband. These interactions respectively contribute to the cooling and heating of the mirror.

Remotely from the mirror, a cloud of atoms is trapped at the overlap of the outgoing Control and the incoming Probe beam. Both the rate and the type of atom-radiation interaction depend sensitively on the atomic parameters. In particular we have demonstrated that, for Λ-level atoms driven in a dark steady-state configuration, the mirror correlation with a specific sideband of the outgoing Control can be converted to that of the incoming Probe. Our main result is the dynamic equation of motional excitation (17).

We have explored two strategies to utilize this atom-modulated mirror-radiation coupling for cooling the mirror. Upon resonant interaction with the blue sideband, the mirror is cooled due to the enhanced BS interaction. However, the motional ground state cannot be reached since TMS heating prevails. On the other hand, TMS heating can be suppressed through resonantly interacting with the red sidebands. With this strategy ground-state cooling is achievable.

Our scheme extends the class of systems that can be optomechanically cooled since neither a high-quality cavity around atoms or mirror is needed, nor precise alignment of incoming and outgoing radiation to form an optical lattice. Moreover, the theoretical tools developed in this work could also be useful to study other radiation-induced interaction between atoms and mirror, such as atom-modulated phonon lasing or atom-mirror entanglement generation.

ACKNOWLEDGMENTS

H.-K.L. thanks Adrian Sanz-Mora and Aashish Clerk for their fruitful discussion. J.-M.R. and A.E. acknowledge support by the Deutsche Forschungsgemeinschaft (DFG) through Grants No. RO 1157/9-1 and No. EI 872/4-1 within the Priority Program SPP 1929 (GiRyd).

APPENDIX A: HAMILTONIAN NEAR MIRROR SURFACE

For self-containedness, we outline the derivation of the cavity-free optomechanical Hamiltonian as follows. Similar system and interaction have also been studied in Refs. [44,45] for generating entanglement between optical field and an isolated vibrating mirror. The total Hamiltonian of the mirror and the radiation field in the vicinity of the mirror surface is given by

$$\frac{H}{\hbar} = \nu\hat{b}^\dagger\hat{b} + \int_{-\infty}^{\infty}\omega_k\hat{a}_k^\dagger\hat{a}_k dk - \frac{A}{\hbar}\hat{q}\left(\frac{\epsilon_0}{2}E(0)^2 + \frac{\mu_0}{2}\mathcal{H}(0)^2\right), \tag{A1}$$

where $\hat{b}$ is the annihilation operator of the mirror motion, $\hat{a}_k$ is the annihilation operator for the light mode with wave vector k, $\omega_k = c|k|$ is the frequency of the mode, A is the cross-section area of the beam, and $\hat{q} = q_0(\hat{b} + \hat{b}^\dagger)$ is the position operator of the mirror. The first and second term of (A1) are the bare Hamiltonians of the mirror motion and radiation field, respectively. The third term is the optomechanical coupling, which is the change of total electromagnetic energy due to the change of radiation space upon mirror displacement. The electric-field and magnetic-field operator at position x is defined by

$$E(x) = \int_{-\infty}^{\infty} i\sqrt{\frac{\hbar\omega_k}{4\pi\epsilon_0 A}}(\hat{a}_k e^{ikx} - \hat{a}_k^\dagger e^{-ikx})\,dk,$$

$$\mathcal{H}(x) = \int_{-\infty}^{\infty} \frac{i}{\mu_0}\sqrt{\frac{\hbar}{4\pi\epsilon_0 A\omega_k}}k(\hat{a}_k e^{ikx} - \hat{a}_k^\dagger e^{-ikx})\,dk.$$

Because the incoming and outgoing radiations are assumed to be almost along the x direction, we can use a scalar k to represent the wave vector of the incoming ($k < 0$) and outgoing ($k > 0$) radiation.

After extracting the contribution of the classical drive, i.e., $\hat{a}_k \to \hat{a}_k + \tilde{\alpha}_p e^{-i\omega_{p0}t}[-\delta(k-k_{p0}) + \delta(k+k_{p0})] + \tilde{\alpha}_c e^{-i\omega_{c0}t}[\delta(k-k_{c0}) - \delta(k+k_{c0})]$, and collecting the quantum contributions up to second order of mode operators, we get the Hamiltonian in (1). Note that this derivation considers only the radiation of one degree of freedom, and so Probe and Control are distinguished by frequency. For Probe and Control that are distinct in other degrees of freedom, e.g., polarization or orbital angular momentum, the Hamiltonian can be derived similarly.

The Hamiltonian in (1) is the starting point of our studies on mirror dynamics. We first directly integrate the Heisenberg equation of the mode operators, i.e., $\dot{\hat{a}}_k = \frac{i}{\hbar}[H, \hat{a}_k]$. By using (3) and the definition (2), we obtain the relations for the incoming field operators:

$$\hat{a}_{-p}(t) = \hat{a}_{-p}^{(1)}(t) + i\tfrac{1}{4}\mu_p(\hat{b}(t) + \hat{b}^\dagger(t)), \tag{A2a}$$

$$\hat{a}_{-c}(t) = \hat{a}_{-c}^{\mathrm{in}}(t) - i\tfrac{1}{4}\mu_c(\hat{b}(t) + \hat{b}^\dagger(t)), \tag{A2b}$$

where $\hat{a}_{-c}^{\text{in}}$ is the Control field input operator from vacuum onto the mirror surface and $\hat{a}_{-p}^{(1)}(t)$ is the Probe field input operator from vacuum through the atomic cloud onto the mirror surface [26]. Because the electric field vanishes on the surface of a perfect conductor, the incoming and outgoing field operators obey the boundary condition

$$\hat{a}_p + \hat{a}_{-p} = \hat{a}_c + \hat{a}_{-c} = 0. \tag{A3}$$

Substituting Eqs. (A2a) and (A3) into the Heisenberg equation of mirror operators, i.e., $\dot{\hat{O}}_b = \frac{i}{\hbar}[H, \hat{O}_b]$, we obtain the Langevin equation (4).

APPENDIX B: ATOMIC DYNAMICS AND STEADY STATE

To study the dynamics of atoms, we arrange the nine atomic operators as an eight-entry vector, i.e., $\vec{\sigma} \equiv (\sigma_{dd} - \sigma_{gg}, \sigma_{ge}, \sigma_{eg}, \sigma_{dd} - \sigma_{ee}, \sigma_{gd}, \sigma_{dg}, \sigma_{ed}, \sigma_{de})^{\mathrm{T}}$, where we have extracted the time invariant $\sigma_{gg} + \sigma_{ee} + \sigma_{dd} = 1$ [46]. The bare dynamics of the atom is described by (7) with no contribution from the mirror and other atoms, i.e., $\hat{a}_{-p}^{(i+1)}$ and $\hat{a}_c^{(i)}$ are taken as vacuum field operators. The expectation value of atomic operators varies as

$$\begin{aligned}
\langle\dot{\sigma}_1^{(i)}\rangle &= -\Gamma_1\langle\sigma_1^{(i)}\rangle - \Gamma_1\langle\sigma_4^{(i)}\rangle - \Omega_p^{(i)*}\langle\sigma_{gd}^{(i)}\rangle - \Omega_p^{(i)}\langle\sigma_{dg}^{(i)}\rangle \\
&\quad - \frac{\Omega_c^{(i)*}}{2}\langle\sigma_{ed}^{(i)}\rangle - \frac{\Omega_c^{(i)}}{2}\langle\sigma_{de}^{(i)}\rangle - \Gamma_1, \\
\langle\dot{\sigma}_{ge}^{(i)}\rangle &= -i(\Delta_g - \Delta_e)\langle\sigma_{ge}^{(i)}\rangle + \frac{\Omega_c^{(i)*}}{2}\langle\sigma_{gd}^{(i)}\rangle + \frac{\Omega_p^{(i)}}{2}\langle\sigma_{de}^{(i)}\rangle, \\
\langle\dot{\sigma}_{eg}^{(i)}\rangle &= i(\Delta_g - \Delta_e)\langle\sigma_{eg}^{(i)}\rangle + \frac{\Omega_c^{(i)}}{2}\langle\sigma_{dg}^{(i)}\rangle + \frac{\Omega_p^{(i)*}}{2}\langle\sigma_{ed}^{(i)}\rangle, \\
\langle\dot{\sigma}_4^{(i)}\rangle &= -\Gamma_4\langle\sigma_1^{(i)}\rangle - \Gamma_4\langle\sigma_4^{(i)}\rangle - \frac{\Omega_p^{(i)*}}{2}\langle\sigma_{gd}^{(i)}\rangle - \frac{\Omega_p^{(i)}}{2}\langle\sigma_{dg}^{(i)}\rangle \\
&\quad - \Omega_c^{(i)*}\langle\sigma_{ed}^{(i)}\rangle - \Omega_c^{(i)}\langle\sigma_{de}^{(i)}\rangle - \Gamma_4, \\
\langle\dot{\sigma}_{gd}^{(i)}\rangle &= \frac{\Omega_p^{(i)}}{2}\langle\sigma_1^{(i)}\rangle - \frac{\Omega_c^{(i)}}{2}\langle\sigma_{ge}^{(i)}\rangle + \left(i\Delta_g - \frac{\tilde{\Gamma}}{2}\right)\langle\sigma_{gd}^{(i)}\rangle, \\
\langle\dot{\sigma}_{dg}^{(i)}\rangle &= \frac{\Omega_p^{(i)*}}{2}\langle\sigma_1^{(i)}\rangle - \frac{\Omega_c^{(i)*}}{2}\langle\sigma_{eg}^{(i)}\rangle + \left(-i\Delta_g - \frac{\tilde{\Gamma}}{2}\right)\langle\sigma_{dg}^{(i)}\rangle, \\
\langle\dot{\sigma}_{ed}^{(i)}\rangle &= -\frac{\Omega_p^{(i)}}{2}\langle\sigma_{eg}^{(i)}\rangle + \frac{\Omega_c^{(i)}}{2}\langle\sigma_4^{(i)}\rangle + \left(-i\Delta_e - \frac{\tilde{\Gamma}}{2}\right)\langle\sigma_{ed}^{(i)}\rangle, \\
\langle\dot{\sigma}_{de}^{(i)}\rangle &= -\frac{\Omega_p^{(i)*}}{2}\langle\sigma_{ge}^{(i)}\rangle + \frac{\Omega_c^{(i)*}}{2}\langle\sigma_4^{(i)}\rangle + \left(i\Delta_e - \frac{\tilde{\Gamma}}{2}\right)\langle\sigma_{de}^{(i)}\rangle,
\end{aligned} \tag{B1}$$

where $\sigma_1 \equiv \sigma_{dd} - \sigma_{gg}$, $\sigma_4 \equiv \sigma_{dd} - \sigma_{ee}$, $\Gamma_1 \equiv \frac{1}{3}(2\gamma_p + 2\Gamma_p + \gamma_c + \Gamma_c)$, $\Gamma_4 \equiv \frac{1}{3}(\gamma_p + \Gamma_p + 2\gamma_c + 2\Gamma_c)$, and $\tilde{\Gamma} \equiv \gamma_p + \Gamma_p + \gamma_c + \Gamma_c$. The above equations are linear, so they can be written in a compact matrix form

$$\langle\dot{\vec{\sigma}}^{(i)}\rangle = \mathbf{M}^{(i)}\langle\vec{\sigma}^{(i)}\rangle + \vec{v}. \tag{B2}$$

The bare steady state can be obtained by setting $\langle\dot{\vec{\sigma}}^{(i)}\rangle_{\mathrm{DS}} = 0$, i.e.,

$$\langle\vec{\sigma}^{(i)}\rangle_{\mathrm{DS}} = -\frac{1}{\mathbf{M}^{(i)}}\vec{v}. \tag{B3}$$

APPENDIX C: COMBINED MASTER EQUATION

After applying the procedures and approximations in the main text, the master equation $\dot{\hat{O}} = \mathcal{L}_b(\hat{O}) + \mathcal{L}_a^{(i)}(\hat{O})$ can be written in a time-local form. The expectation value of any system operator in the form of $\hat{O}_b$ or $\vec{O} \equiv \hat{O}_b \otimes \vec{\sigma}^{(i)}$ varies as

$$\begin{aligned}
\langle\dot{\hat{O}}_b\rangle &= i\nu\langle[\hat{b}^\dagger\hat{b}, \hat{O}_b]\rangle + \frac{|\mu_p|^2 + |\mu_c|^2}{2}\langle\mathcal{D}[\hat{b} + \hat{b}^\dagger](\hat{O}_b)\rangle \\
&\quad - i\mu_p\langle\mathcal{A}_p^{(1)\dagger}[\hat{b} + \hat{b}^\dagger, \hat{O}_b]\rangle - i\mu_p^*\langle[\hat{b} + \hat{b}^\dagger, \hat{O}_b]\mathcal{A}_p^{(1)}\rangle,
\end{aligned} \tag{C1}$$

$$\begin{aligned}
\langle\dot{\vec{O}}\rangle &= i\nu\langle[\hat{b}^\dagger\hat{b}, \vec{O}]\rangle + \frac{|\mu_p|^2 + |\mu_c|^2}{2}\langle\mathcal{D}[\hat{b} + \hat{b}^\dagger](\vec{O})\rangle \\
&\quad - i\mu_p\langle\mathcal{A}_p^{(1)\dagger}[\hat{b} + \hat{b}^\dagger, \vec{O}]\rangle - i\mu_p^*\langle[\hat{b} + \hat{b}^\dagger, \vec{O}]\mathcal{A}_p^{(1)}\rangle \\
&\quad + \mathbf{M}^{(i)}\langle\vec{O}\rangle + \langle\hat{O}_b\rangle\vec{v} - \sqrt{\gamma_p}\Big(e^{i\omega_{p0}\frac{x_i}{c}}\mathbf{M}_{pd}\langle\mathcal{A}_p^{(i+1)\dagger}\vec{O}\rangle \\
&\quad - e^{-i\omega_{p0}\frac{x_i}{c}}\mathbf{M}_p\langle\vec{O}\mathcal{A}_p^{(i+1)}\rangle\Big) \\
&\quad - \sqrt{\gamma_c}\Big(e^{-i\omega_{c0}\frac{x_i}{c}}\mathbf{M}_{cd}\langle\mathcal{A}_c^{(i)\dagger}\vec{O}\rangle - e^{i\omega_{c0}\frac{x_i}{c}}\mathbf{M}_c\langle\vec{O}\mathcal{A}_c^{(i)}\rangle\Big) \\
&\quad + i\frac{\sqrt{\gamma_c}}{2}\Big(\mu_c^* e^{-i\omega_{c0}\frac{x_i}{c}}\mathbf{M}_{cd}\langle(e^{i\nu\tau}\hat{b} + e^{-i\nu\tau}\hat{b}^\dagger)\vec{O}\rangle \\
&\quad + \mu_c e^{i\omega_{c0}\frac{x_i}{c}}\mathbf{M}_c\langle\vec{O}(e^{i\nu\tau}\hat{b} + e^{-i\nu\tau}\hat{b}^\dagger)\rangle\Big).
\end{aligned} \tag{C2}$$

The transformation matrices are defined as $\mathbf{M}_{pd}\vec{\sigma} \equiv [\sigma_{gd}, \vec{\sigma}]$, $\mathbf{M}_p\vec{\sigma} \equiv [\sigma_{dg}, \vec{\sigma}]$, $\mathbf{M}_{cd}\vec{\sigma} \equiv [\sigma_{ed}, \vec{\sigma}]$, and $\mathbf{M}_c\vec{\sigma} \equiv [\sigma_{de}, \vec{\sigma}]$, i.e.,

$$\mathbf{M}_{pd} = \begin{pmatrix}
0 & 0 & 0 & 0 & 2 & 0 & 0 & 0 \\
0 & 0 & 0 & 0 & 0 & 0 & 0 & 0 \\
0 & 0 & 0 & 0 & 0 & 0 & -1 & 0 \\
0 & 0 & 0 & 0 & 1 & 0 & 0 & 0 \\
0 & 0 & 0 & 0 & 0 & 0 & 0 & 0 \\
-1 & 0 & 0 & 0 & 0 & 0 & 0 & 0 \\
0 & 0 & 0 & 0 & 0 & 0 & 0 & 0 \\
0 & 1 & 0 & 0 & 0 & 0 & 0 & 0
\end{pmatrix}, \tag{C3}$$

$$\mathbf{M}_p = \begin{pmatrix}
0 & 0 & 0 & 0 & 0 & -2 & 0 & 0 \\
0 & 0 & 0 & 0 & 0 & 0 & 0 & 1 \\
0 & 0 & 0 & 0 & 0 & 0 & 0 & 0 \\
0 & 0 & 0 & 0 & 0 & -1 & 0 & 0 \\
1 & 0 & 0 & 0 & 0 & 0 & 0 & 0 \\
0 & 0 & 0 & 0 & 0 & 0 & 0 & 0 \\
0 & 0 & -1 & 0 & 0 & 0 & 0 & 0 \\
0 & 0 & 0 & 0 & 0 & 0 & 0 & 0
\end{pmatrix}, \tag{C4}$$

$$\mathbf{M}_{cd} = \begin{pmatrix}
0 & 0 & 0 & 0 & 0 & 0 & 1 & 0 \\
0 & 0 & 0 & 0 & -1 & 0 & 0 & 0 \\
0 & 0 & 0 & 0 & 0 & 0 & 0 & 0 \\
0 & 0 & 0 & 0 & 0 & 0 & 2 & 0 \\
0 & 0 & 0 & 0 & 0 & 0 & 0 & 0 \\
0 & 0 & 1 & 0 & 0 & 0 & 0 & 0 \\
0 & 0 & 0 & 0 & 0 & 0 & 0 & 0 \\
0 & 0 & 0 & -1 & 0 & 0 & 0 & 0
\end{pmatrix}, \tag{C5}$$

$$\mathbf{M}_c = \begin{pmatrix} 0 & 0 & 0 & 0 & 0 & 0 & 0 & -1 \\ 0 & 0 & 0 & 0 & 0 & 0 & 0 & 0 \\ 0 & 0 & 0 & 0 & 0 & 1 & 0 & 0 \\ 0 & 0 & 0 & 0 & 0 & 0 & 0 & -2 \\ 0 & -1 & 0 & 0 & 0 & 0 & 0 & 0 \\ 0 & 0 & 0 & 0 & 0 & 0 & 0 & 0 \\ 0 & 0 & 0 & 1 & 0 & 0 & 0 & 0 \\ 0 & 0 & 0 & 0 & 0 & 0 & 0 & 0 \end{pmatrix}. \tag{C6}$$

We have assumed that the input fields of Probe, Control, and baths are vacuum, i.e., $\hat{a}^{\rm in}_{\pm\beta}|{\rm vac}\rangle = \hat{r}^{\rm in}_{\beta}|{\rm vac}\rangle = 0$, for β could be p or c. The round-trip traveling time of radiation between the mirror (at $x = 0$) and atomic cloud (mean location $x = \bar{x}$) is $\tau \equiv 2\bar{x}/c$. The tilde for the advanced operators has been omitted.

APPENDIX D: DERIVATION OF RECURRENCE RELATION

To derive the recurrence relation in Eqs. (12a)–(12d), we start by using (C2)) for $\vec{O} = \hat{b} \otimes \vec{\sigma}$ and $\hat{b}^\dagger \otimes \vec{\sigma}$. We apply the steady-state approximation $\sigma \approx \langle {\rm DS}|\sigma|{\rm DS}\rangle$, and collect only the leading-order quantum correction of atomic operators. Then we get the following relations for the zero-frequency components:

$$\begin{aligned} 2\pi\langle \hat{b}\sigma^{(i)}_{gd}\rangle_0 = &-\sqrt{\gamma_p}\Big(e^{i\omega_{p0}\frac{x_i}{c}}G^{(i)}_{pd}(-\nu)\langle \hat{b}\mathcal{A}^{(i+1)\dagger}_p\rangle_0 - e^{-i\omega_{p0}\frac{x_i}{c}}G^{(i)}_{p}(-\nu)\langle \hat{b}\mathcal{A}^{(i+1)}_p\rangle_0\Big) \\ &-\sqrt{\gamma_c}\Big(e^{-i\omega_{c0}\frac{x_i}{c}}G^{(i)}_{cd}(-\nu)\langle \hat{b}\mathcal{A}^{(i)\dagger}_c\rangle_0 - e^{i\omega_{c0}\frac{x_i}{c}}G^{(i)}_{c}(-\nu)\langle \hat{b}\mathcal{A}^{(i)}_c\rangle_0\Big) \\ &+i\frac{\sqrt{\gamma_c}}{2}\Big(e^{-i\nu\tau}\mu_c^* e^{-i\omega_{c0}\frac{x_i}{c}}G^{(i)}_{cd}(-\nu)\langle \hat{b}^\dagger\hat{b}\rangle + e^{-i\nu\tau}\mu_c e^{i\omega_{c0}\frac{x_i}{c}}G^{(i)}_{c}(-\nu)\langle \hat{b}\hat{b}^\dagger\rangle\Big), \end{aligned} \tag{D1}$$

$$\begin{aligned} 2\pi\langle \hat{b}^\dagger\sigma^{(i)}_{gd}\rangle_0 = &-\sqrt{\gamma_p}\Big(e^{i\omega_{p0}\frac{x_i}{c}}G^{(i)}_{pd}(\nu)\langle \hat{b}^\dagger\mathcal{A}^{(i+1)\dagger}_p\rangle_0 - e^{-i\omega_{p0}\frac{x_i}{c}}G^{(i)}_{p}(\nu)\langle \hat{b}^\dagger\mathcal{A}^{(i+1)}_p\rangle_0\Big) \\ &-\sqrt{\gamma_c}\Big(e^{-i\omega_{c0}\frac{x_i}{c}}G^{(i)}_{cd}(\nu)\langle \hat{b}^\dagger\mathcal{A}^{(i)\dagger}_c\rangle_0 - e^{i\omega_{c0}\frac{x_i}{c}}G^{(i)}_{c}(\nu)\langle \hat{b}^\dagger\mathcal{A}^{(i)}_c\rangle_0\Big) \\ &+i\frac{\sqrt{\gamma_c}}{2}\Big(e^{i\nu\tau}\mu_c^* e^{-i\omega_{c0}\frac{x_i}{c}}G^{(i)}_{cd}(\nu)\langle \hat{b}\hat{b}^\dagger\rangle + e^{i\nu\tau}\mu_c e^{i\omega_{c0}\frac{x_i}{c}}G^{(i)}_{c}(\nu)\langle \hat{b}^\dagger\hat{b}\rangle\Big), \end{aligned} \tag{D2}$$

$$\begin{aligned} 2\pi\langle \hat{b}\sigma^{(i)}_{ed}\rangle_0 = &-\sqrt{\gamma_p}\Big(e^{i\omega_{p0}\frac{x_i}{c}}F^{(i)}_{pd}(-\nu)\langle \hat{b}\mathcal{A}^{(i+1)\dagger}_p\rangle_0 - e^{-i\omega_{p0}\frac{x_i}{c}}F^{(i)}_{p}(-\nu)\langle \hat{b}\mathcal{A}^{(i+1)}_p\rangle_0\Big) \\ &-\sqrt{\gamma_c}\Big(e^{-i\omega_{c0}\frac{x_i}{c}}F^{(i)}_{cd}(-\nu)\langle \hat{b}\mathcal{A}^{(i)\dagger}_c\rangle_0 - e^{i\omega_{c0}\frac{x_i}{c}}F^{(i)}_{c}(-\nu)\langle \hat{b}\mathcal{A}^{(i)}_c\rangle_0\Big) \\ &+i\frac{\sqrt{\gamma_c}}{2}\Big(e^{-i\nu\tau}\mu_c^* e^{-i\omega_{c0}\frac{x_i}{c}}F^{(i)}_{cd}(-\nu)\langle \hat{b}^\dagger\hat{b}\rangle + e^{-i\nu\tau}\mu_c e^{i\omega_{c0}\frac{x_i}{c}}F^{(i)}_{c}(-\nu)\langle \hat{b}\hat{b}^\dagger\rangle\Big), \end{aligned} \tag{D3}$$

$$\begin{aligned} 2\pi\langle \hat{b}^\dagger\sigma^{(i)}_{ed}\rangle_0 = &-\sqrt{\gamma_p}(e^{i\omega_{p0}\frac{x_i}{c}}F^{(i)}_{pd}(\nu)\langle \hat{b}^\dagger\mathcal{A}^{(i+1)\dagger}_p\rangle_0 - e^{-i\omega_{p0}\frac{x_i}{c}}F^{(i)}_{p}(\nu)\langle \hat{b}^\dagger\mathcal{A}^{(i+1)}_p\rangle_0) \\ &-\sqrt{\gamma_c}(e^{-i\omega_{c0}\frac{x_i}{c}}F^{(i)}_{cd}(\nu)\langle \hat{b}^\dagger\mathcal{A}^{(i)\dagger}_c\rangle_0 - e^{i\omega_{c0}\frac{x_i}{c}}F^{(i)}_{c}(\nu)\langle \hat{b}^\dagger\mathcal{A}^{(i)}_c\rangle_0) \\ &+i\frac{\sqrt{\gamma_c}}{2}\Big(e^{i\nu\tau}\mu_c^* e^{-i\omega_{c0}\frac{x_i}{c}}F^{(i)}_{cd}(\nu)\langle \hat{b}\hat{b}^\dagger\rangle + e^{i\nu\tau}\mu_c e^{i\omega_{c0}\frac{x_i}{c}}F^{(i)}_{c}(\nu)\langle \hat{b}^\dagger\hat{b}\rangle\Big), \end{aligned} \tag{D4}$$

where

$$G^{(i)}_y(\omega) \equiv 2\pi\hat{u}_5 \cdot \frac{-1}{i\omega + \mathbf{M}^{(i)}}\mathbf{M}_y\langle {\rm DS}^{(i)}|\vec{\sigma}^{(i)}|{\rm DS}^{(i)}\rangle, \tag{D5}$$

$$F^{(i)}_y(\omega) \equiv 2\pi\hat{u}_7 \cdot \frac{-1}{i\omega + \mathbf{M}^{(i)}}\mathbf{M}_y\langle {\rm DS}^{(i)}|\vec{\sigma}^{(i)}|{\rm DS}^{(i)}\rangle, \tag{D6}$$

for $y = p,\ pd,\ c$, or cd. The projection vectors are defined as $\hat{u}_5 \equiv (0\,0\,0\,0\,1\,0\,0\,0)$ and $\hat{u}_7 \equiv (0\,0\,0\,0\,0\,0\,1\,0)$, such that $\hat{u}_5 \cdot \vec{\sigma} = \sigma_{gd}$ and $\hat{u}_7 \cdot \vec{\sigma} = \sigma_{ed}$.

Evaluating Eqs. (D5) and (D6), we find that $G_{pd} = G_{cd} = F_{pd} = F_{cd} = 0$, and

$$G^{(i)}_p(\omega) = |\tilde{\alpha}_c|^2\frac{2\pi}{\gamma_p}J(\omega), \tag{D7}$$

$$G^{(i)}_c(\omega) = -e^{-i(\omega_{p0}+\omega_{c0})\frac{x_i}{c}}\tilde{\alpha}_p\tilde{\alpha}_c^*\frac{2\pi}{\sqrt{\gamma_p\gamma_c}}J(\omega), \tag{D8}$$

$$F^{(i)}_p(\omega) = -e^{i(\omega_{p0}+\omega_{c0})\frac{x_i}{c}}\tilde{\alpha}_p^*\tilde{\alpha}_c\frac{2\pi}{\sqrt{\gamma_p\gamma_c}}J(\omega), \tag{D9}$$

$$F^{(i)}_c(\omega) = |\tilde{\alpha}_p|^2\frac{2\pi}{\gamma_c}J(\omega), \tag{D10}$$

where $J(\omega)$ is given in (13). The recurrence relation Eqs. (12a) and (12b) can be obtained by using the definitions $\mathcal{A}^{(i)}_p - \mathcal{A}^{(i+1)}_p = \sqrt{\gamma_p}e^{i\omega_{p0}\frac{x_i}{c}}\sigma^{(i)}_{gd}$ and $\mathcal{A}^{(i+1)}_c - \mathcal{A}^{(i)}_c = \sqrt{\gamma_c}e^{-i\omega_{c0}\frac{x_i}{c}}\sigma^{(i)}_{ed}$.

APPENDIX E: SOLUTION OF RECURRENCE RELATION

To obtain the value of $\langle \hat{b}\mathcal{A}^{(1)}_p\rangle_0$ from the recurrence relation Eqs. (12a) and (12b), we consider the sum of these equations, that is the relation in (14). This relation implies that the properties at the ends of the atomic cloud are related as

$$\begin{aligned} \langle \hat{b}\mathcal{A}^{(1)}_p\rangle_0 - \langle \hat{b}\mathcal{A}^{(1)}_c\rangle_0 &= \langle \hat{b}\mathcal{A}^{(i)}_p\rangle_0 - \langle \hat{b}\mathcal{A}^{(i)}_c\rangle_0 \\ &= \langle \hat{b}\mathcal{A}^{(N+1)}_p\rangle_0 - \langle \hat{b}\mathcal{A}^{(N+1)}_c\rangle_0. \end{aligned} \tag{E1}$$

We also consider the difference of Eqs. (12a) and (12b), which gives the following relation:

$$\begin{aligned}&\langle\hat{b}\mathcal{A}_p^{(i+1)}\rangle_0+\langle\hat{b}\mathcal{A}_c^{(i+1)}\rangle_0\\&\approx\langle\hat{b}\mathcal{A}_p^{(i)}\rangle_0+\langle\hat{b}\mathcal{A}_c^{(i)}\rangle_0-2|\tilde{\alpha}|^2J(-\nu)\big(\langle\hat{b}\mathcal{A}_p^{(i)}\rangle_0-\langle\hat{b}\mathcal{A}_c^{(i)}\rangle_0\big)\\&\quad+ie^{-i\nu\tau}\mu_c|\tilde{\alpha}|^2J(-\nu)\langle\hat{b}\hat{b}^\dagger\rangle.\end{aligned}\tag{E2}$$

We have collected only the leading order of the small factor $|\tilde{\alpha}|^2|J(\omega)|\ll 1$, which is valid because each atom is weakly interacting with quantum radiation. By repeating (E2) from $i=1$ to $i=N$, and using (E1), we get another relation for the properties at the ends of the atomic cloud

$$\begin{aligned}&\langle\hat{b}\mathcal{A}_p^{(N+1)}\rangle_0+\langle\hat{b}\mathcal{A}_c^{(N+1)}\rangle_0\\&=(1-2N|\tilde{\alpha}|^2J(-\nu))\langle\hat{b}\mathcal{A}_p^{(1)}\rangle_0\\&\quad+(1+2N|\tilde{\alpha}|^2J(-\nu))\langle\hat{b}\mathcal{A}_c^{(1)}\rangle_0\\&\quad+ie^{-i\nu\tau}\mu_cN|\tilde{\alpha}|^2J(-\nu)\langle\hat{b}\hat{b}^\dagger\rangle.\end{aligned}\tag{E3}$$

Combining Eqs. (E1) and (E3) to eliminate $\langle\hat{b}\mathcal{A}_c^{(N+1)}\rangle_0$, and using the definition $\mathcal{A}_p^{(N+1)}=\mathcal{A}_c^{(1)}=0$, we obtain the solution in (16a). Equation (16b) can be obtained through similar procedures.

APPENDIX F: UNEQUAL DRIVING AMPLITUDE

In Sec. V we have calculated the cooling rate for the case with equal driving amplitude, i.e., $\tilde{\alpha}_p=\tilde{\alpha}_c$. For general amplitudes, Eqs. (12a)–(12d) can also be solved analytically. The result remains Eqs. (16a) and (16b), but $\mathcal{S}(\omega)$ becomes

$$\mathcal{S}(\omega)=-\frac{\tilde{\alpha}_c^*}{\alpha_p^*}\left(\frac{|\tilde{\alpha}_p|^2-|\tilde{\alpha}_p|^2e^{NJ(\omega)(|\tilde{\alpha}_p|^2-|\tilde{\alpha}_c|^2)}}{|\tilde{\alpha}_p|^2-|\tilde{\alpha}_c|^2e^{NJ(\omega)(|\tilde{\alpha}_p|^2-|\tilde{\alpha}_c|^2)}}\right).\tag{F1}$$

It is easy to check that Eq. (16c) is recovered when taking the limit $\tilde{\alpha}_p\to\tilde{\alpha}_c$. The atom-induced cooling rate follows the definition in Eq. (18).

For the cooling strategy of enhancing BS effect, we find that the steady-state motional excitation in the many-atom regime is lower bounded by

$$\langle\hat{n}\rangle_{\rm ss}\geqslant\frac{\max\{|\tilde{\alpha}_p|,|\tilde{\alpha}_c|\}}{\min\{|\tilde{\alpha}_p|,|\tilde{\alpha}_c|\}}\geqslant 1.\tag{F2}$$

The last relation, which is equivalent to Eq. (22), can be saturated by choosing $\tilde{\alpha}_p=\tilde{\alpha}_c$ and $\mu_p=\mu_c$.

For the cooling strategy of suppressing TMS heating effect, we find that the steady-state motional excitation in the many-atom regime is lower bounded by

$$\langle\hat{n}\rangle_{\rm ss}\geqslant\frac{\max\{|\tilde{\alpha}_p|,|\tilde{\alpha}_c|\}}{\min\{|\tilde{\alpha}_p|,|\tilde{\alpha}_c|\}}-1\geqslant 0.\tag{F3}$$

The last relation, which is equivalent to Eq. (24) and represents ground-state cooling, is attainable by choosing $\tilde{\alpha}_p=\tilde{\alpha}_c$ and $\mu_p=\mu_c$.

[1] C. M. Caves, Phys. Rev. Lett. **45**, 75 (1980).
[2] V. B. Braginsky, V. P. Mitrofanov, and K. V. Tokmakov, Phys. Lett. A **218**, 164 (1996).
[3] V. B. Braginsky, M. L. Gorodetsky, and F. Y. Khalili, Phys. Lett. A **232**, 340 (1997).
[4] S. Rowan, S. M. Twyford, R. Hutchins, J. Kovalik, J. E. Logan, A. C. McLaren, N. A. Robertson, and J. Hough, Phys. Lett. A **233**, 303 (1997).
[5] I. Pikovski, M. R. Vanner, M. Aspelmeyer, M. S. Kim, and Č. Brukner, Nat. Phys. **8**, 393 (2012).
[6] W. Marshall, C. Simon, R. Penrose, and D. Bouwmeester, Phys. Rev. Lett. **91**, 130401 (2003).
[7] P. Rabl, S. J. Kolkowitz, F. H. L. Koppens, J. G. E. Harris, P. Zoller, and M. D. Lukin, Nat. Phys. **6**, 602 (2010).
[8] S. Rips and M. J. Hartmann, Phys. Rev. Lett. **110**, 120503 (2013).
[9] M. Poot and H. S. J. van der Zant, Phys. Rep. **511**, 273 (2012).
[10] M. Aspelmeyer, P. Meystre, and K. Schwab, Phys. Today **65**(7), 29 (2012).
[11] F. Pobell, *Matter and Methods at Low Temperatures* (Springer, New York, 2007).
[12] I. Wilson-Rae, N. Nooshi, W. Zwerger, and T. J. Kippenberg, Phys. Rev. Lett. **99**, 093901 (2007).
[13] F. Marquardt, J. P. Chen, A. A. Clerk, and S. M. Girvin, Phys. Rev. Lett. **99**, 093902 (2007).
[14] M. Aspelmeyer, T. J. Kippenberg, and F. Marquardt, Rev. Mod. Phys. **86**, 1391 (2014).
[15] R. Rivière, S. Deléglise, S. Weis, E. Gavartin, O. Arcizet, A. Schliesser, and T. J. Kippenberg, Phys. Rev. A **83**, 063835 (2011).
[16] A. Sawadsky, H. Kaufer, R. M. Nia, S. P. Tarabrin, F. Y. Khalili, K. Hammerer, and R. Schnabel, Phys. Rev. Lett. **114**, 043601 (2015).
[17] J. D. Teufel, T. Donner, D. Li, J. W. Harlow, M. S. Allman, K. Cicak, A. J. Sirois, J. D. Whittaker, K. W. Lehnert, and R. W. Simmonds, Nature (London) **475**, 359 (2011).
[18] J. Chan, T. P. M. Alegre, A. H. Safavi-Naeini, J. T. Hill, A. Krause, S. Gröblacher, M. Aspelmeyer, and O. Painter, Nature (London) **478**, 89 (2011).
[19] K. Hammerer, K. Stannigel, C. Genes, P. Zoller, P. Treutlein, S. Camerer, D. Hunger, and T. W. Hänsch, Phys. Rev. A **82**, 021803(R) (2010).
[20] S. Camerer, M. Korppi, A. Jockel, D. Hunger, T. W. Hänsch, and P. Treutlein, Phys. Rev. Lett. **107**, 223001 (2011).
[21] B. Vogell, K. Stannigel, P. Zoller, K. Hammerer, M. T. Rakher, M. Korppi, A. Jöckel, and P. Treutlein, Phys. Rev. A **87**, 023816 (2013).
[22] B. Vogell, T. Kampschulte, M. T. Rakher, A. Faber, P. Treutlein, K. Hammerer, and P. Zoller, New J. Phys. **17**, 043044 (2015).

[23] A. Vochezer, T. Kampschulte, K. Hammerer, and P. Treutlein, Phys. Rev. Lett. **120**, 073602 (2018).
[24] A. Sanz-Mora, A. Eisfeld, S. Wüster, and J.-M. Rost, Phys. Rev. A **93**, 023816 (2016).
[25] C. Weedbrook, S. Pirandola, R. García-Patrón, N. J. Cerf, T. C. Ralph, J. H. Shapiro, and S. Lloyd, Rev. Mod. Phys. **84**, 621 (2012).
[26] C. W. Gardiner and P. Zoller, *Quantum Noise: A Handbook of Markovian and Non-Markovian Quantum Stochastic Methods with Applications to Quantum Optics* (Springer, New York, 2004).
[27] G. Morigi, J. Eschner, and C. H. Keitel, Phys. Rev. Lett. **85**, 4458 (2000).
[28] G. Morigi, Phys. Rev. A **67**, 033402 (2003).
[29] We note that this criterion does not contradict our assumption that Probe and Control mode frequencies are sufficiently separated. It is because Probe and Control can be treated as two separate continuum if their frequency difference is much wider than oscillation frequency ν, which is orders of magnitude smaller than the optical frequency of radiation. Furthermore, Probe and Control can be distinct by other degrees of freedom, such as polarization.
[30] J. B. Clark, F. Lecocq, R. W. Simmonds, J. Aumentado, and J. D. Teufel, Nature (London) **541**, 191 (2017).
[31] M. Asjad, S. Zippilli, and D. Vitali, Phys. Rev. A **94**, 051801(R) (2016).
[32] C. Schäfermeier, H. Kerdoncuff, U. B. Hoff, H. Fu, A. Huck, J. Bilek, G. I. Harris, W. P. Bowen, T. Gehring, and U. L. Andersen, Nat. Commun. **7**, 13628 (2016).
[33] F. Elste, S. M. Girvin, and A. A. Clerk, Phys. Rev. Lett. **102**, 207209 (2009).
[34] C. Genes, H. Ritsch, and D. Vitali, Phys. Rev. A **80**, 061803(R) (2009).
[35] C. Genes, H. Ritsch, M. Drewsen, and A. Dantan, Phys. Rev. A **84**, 051801(R) (2011).
[36] A. Dantan, B. Nair, G. Pupillo, and C. Genes, Phys. Rev. A **90**, 033820 (2014).
[37] C. G. Ondřej Černotík and A. Dantan, arXiv:1809.01420.
[38] A. Xuereb, R. Schnabel, and K. Hammerer, Phys. Rev. Lett. **107**, 213604 (2011).
[39] T. Ojanen and K. Børkje, Phys. Rev. A **90**, 013824 (2014).
[40] Y. Tao, J. M. Boss, B. A. Moores, and C. L. Degen, Nat. Commun. **5**, 3638 (2014).
[41] D. A. Steck, Rubidium 85 D Line Data, available online at http://steck.us/alkalidata (revision 2.1.6), 2013.
[42] P. Marek, L. Lachman, L. Slodička, and R. Filip, Phys. Rev. A **94**, 013850 (2016).
[43] H.-K. Lau and M. B. Plenio, Phys. Rev. A **95**, 022303 (2017).
[44] S. Mancini, D. Vitali, and P. Tombesi, Phys. Rev. Lett. **90**, 137901 (2003).
[45] S. Pirandola, S. Mancini, D. Vitali, and P. Tombesi, Phys. Rev. A **68**, 062317 (2003).
[46] H.-K. Lau and M. B. Plenio, Phys. Rev. B **94**, 054305 (2016).